



## COVER SHEET

---

Ford, Jason J. and Ledwich, G and Dong, Z.Y. (2006) Nonlinear Control of Single-Machine-Infinite-Bus Transient Stability. In *Proceedings Power Engineering Society General Meeting, 2006*, pages pp. 1-8.

Accessed from <http://eprints.qut.edu.au>

Copyright 2006 IEEE.

# Nonlinear Control of Single-Machine-Infinite-Bus Transient Stability

J.J. Ford, G. Ledwich *Senior Member, IEEE*, and Z.Y. Dong *Member, IEEE*

**Abstract**—Of increasing importance in network design is the requirement to control power system transient stability following large disturbances. If series or shunt control devices are available within the network, then improvements to the transient properties of the network can generally be made (both from the perspective of preventing angular separation and improving damping).

This paper uses non-linear control (dynamic programming) to examine the transient stability problem for single machine infinite bus systems. The developed approach explains the suitability of several existing approaches, as well as identifies some new ideas that may be applicable to the transient stability problem for multi-generator power systems.

**Index Terms**—Optimal Control, Dynamic Programming, Power System Transient Stability, and Switching Systems.

## I. INTRODUCTION

Electric power generation and supply grids are becoming more complicated and stressed due to increasing demands for efficiency and reliability [6]. Operating power generation systems closer to their capacity limits, with improved reliability, will require the improved application of advanced control technologies.

The necessary advanced technologies not only includes advanced series and shunt variable capacitance control devices [10] but also advanced actuation and sensing technologies and advanced control analysis and synthesis tools [14], [4], [6], [7], [8].

This paper focuses on the application of these advanced technologies to transient stability problems following large disturbances, with a particular interest in extreme cases. The simplest transient stability control problem is the proto-type problem for single machine infinite bus (SMIB) systems.

Previously, time-optimal control approaches have been used to solve the SMIB transient stability problem (and these approaches lead to bang-bang type control strategies) [7], [4], [8]. There are several features of these time-optimal control solutions that are worth noting.

Firstly, the time-optimal approach has attracted some level of attention because, in the SMIB case, it leads to solutions that can be expressed in an analytic form in terms of switching curves in a phase-plane [11]. In particular, using the maximum

principle of optimal control, previous work has shown that the time-optimal control can be described either by a single switching curve [4] or by multiple switching curves [8].

Secondly, the bang-bang nature of these controllers has been accepted as reasonable during periods of large risk of angular separation [14], but bang-bang controllers are not the most desirable method for damping the system dynamics when there is a small risk of separation (due to secondary concerns about power quality effects such as voltage flicker and other non-linear effects). Therefore, while the time-optimal performance objective somewhat matches the intuition that fast stabilisation is desirable, it is more reasonable to represent the real performance objectives as a mixture of separation issues and power quality issues.

Also of interest, several sub-optimal approaches have recently been proposed that are based on switching on, or near, the  $\omega = 0$  line (termed velocity controllers). A better understanding of the stability properties of these controllers is desired.

The main contribution of this paper is to rigorously re-examine the SMIB transient stability problem within a non-linear optimal control framework that allows general performance criteria. Our aim is to develop an improved understanding of the transient stability problem. This examination allows us to compare and contrast previously proposed solutions within the one framework and allows us to confirm existing ideas and to identify some new important concepts.

Over the last decade, the control community has developed several suitable numeric techniques for the dynamic programming approach to non-linear optimal control. These numeric approaches are now well established (see [3]) and ensure that the dynamic programming approach is feasible (admittedly, only for small order models and not scalable to realistic multi-generator power systems).

In this paper we use the dynamic programming approach for optimal control to propose advanced control designs that better reflect power system design objectives (admittedly, *i priori*, we might expect the solutions to be more complicated). We present the general optimal control solution (described by partial differential equations) and then illustrate a numeric design procedure that can be used to solve a variety of transient control problems.

Several examples are provided that illustrate the nature of the optimal solution to the SMIB transient stability problem. In particular, these examples are selected to provide further support for some previously developed approaches (such as the sub-optimal velocity controller [13], [14]), but also to highlight some features of the problem that have not previously been

This work was supported by the Australian Research Council.

J.J. Ford is with the School of Engineering Systems, Queensland University of Technology, GPO Box 2434 Brisbane, QLD 4001, Australia. (e-mail: j2.ford@qut.edu.au)

G. Ledwich is with the School of Engineering Systems, Queensland University of Technology, GPO Box 2434 Brisbane, QLD 4001, Australia.

Z.Y. Dong is with the School of Information Technology and Electrical Engineering, The University of Queensland, St Lucia, QLD 4072, Australia.

identified.

This paper is structured as follows: In Section II, a SMIB dynamic model is presented. In Section III, an appropriate non-linear optimal control framework is introduced, solutions are presented, and numeric techniques briefly discussed. In Section IV, optimal solutions to various transient stability problems (for several different criteria) are calculated and discussed. Finally, in Section V, some conclusions are provided.

## II. DYNAMICS

This section presents a model of SMIB transient dynamics following large disturbances (faults). We will assume that prior to the fault the system was in equilibrium (ie.  $\dot{\omega} = 0$ ,  $\omega = 0$  and  $\delta = \delta_s$ ). We assume that the fault continues until cleared at time  $t_c$ . At this point, the power generation system enters a post fault period, beginning at a non-equilibrium condition, during which the machine is at risk of angular separation from an infinite bus.

Because we are primarily concerned with the short-term dynamic stability problem, we will consider the classic post-fault SMIB generator model. We will assume that series or shunt compensation devices are installed in the network and can be used to change network parameters, in this case the network impedances.

In the classic SMIB model, the generator rotor dynamics are described by

$$\begin{aligned} \dot{\delta} &= \omega \\ M\dot{\omega} &= P_m - P_{max}(u) \sin(\delta) \end{aligned} \quad (1)$$

where  $\delta$  is the rotor angle measure with respect to the angle of the infinite bus,  $\omega$  is the angular speed,  $P_m$  is the mechanical power supplier to the generator,  $P_{max}(u)$  is the maximum electrical power that can be supplied by the generator, and  $u$  is a control action that is to be designed.

Assuming constant frequency and ignoring line resistances, the maximum electrical power is given by

$$P_{max}(u) = \frac{|E||V|}{X_{eff}(u)}$$

where  $E$  is the internal generator voltage,  $V$  is the infinite bus voltage and  $X_{eff}(u)$  is the equivalent admittance of the line between the generator and the bus (including transformer and internal generator impedances, under the control action  $u$ ).

This SMIB model is often used in power system transient stability analysis [5], [6]. In particular, the extended equal area criterion (EEAC) for multi-machine system analysis is based on a version of the SMIB model [5], [6], [14]. This observation highlights that understanding the stability properties of the SMIB systems has significance in multi-generator stability analysis.

Admittedly, the classical SMIB type analysis ignores higher-order dynamics that may be important in the context of other stability or design issues (for example, fast or ‘‘chattering’’ type controls near the system equilibrium points, although unrepresented in this model, are certainly undesirable).

*Remarks:*

- 1) For simplicity of presentation we have assumed no damping term. The presentation that follows can be suitably modified to handle power generator dynamics containing damping terms without any significant impact on the presented approach.
- 2) A number of the assumptions are necessary to ensure a lower order dynamic model (for example, constant electrical frequency assumptions, connection to infinite bus assumptions, the 2nd-order generator dynamics and constant load impedance assumptions). Each or any of these assumptions could be relaxed at the expense of increasing the order of the dynamic model and hence the numeric difficulty.

## III. OPTIMAL CONTROL AND STABILITY RESULTS

### A. Optimal Control Framework

To consider our transient stability problem within an optimal control framework, we introduce the following state-based model description. As shorthand, let us denote the state of the SMIB by  $x = [\delta, \omega]'$  and the dynamics by

$$f(x, u) = \begin{bmatrix} x_2 \\ M^{-1}(P_m - P_{max}(u) \sin(x_1)) \end{bmatrix}$$

where  $x_i$  denotes the  $i$ th element of  $x$ . We assume  $u \in \mathcal{U}$  where  $\mathcal{U}$  is a (possibly finite) set of possible (switch) control values. We will require  $\mathcal{U}$  to be a closed bounded set where  $u_{min}$  and  $u_{max}$  are the smallest and largest members, respectively.

Then we can consider the SMIB transient stability problem as having the following non-linear description:

$$\dot{x} = f(x, u). \quad (2)$$

In this paper, we will consider SMIB dynamics that begin at  $t = t_c$  (the fault clearance time) from location  $x_0$ . From a control perspective, the post-fault problem depends only on the initial post-fault state and the post-fault system parameters (in particular, it is independent of the state trajectory followed during the fault).

This ‘‘fault-independent’’ approach is conceptually different from previous approaches to the control of transient dynamics (such as [4], [8], [14] and others) in which the nature of fault trajectories is, either implicitly or explicitly, incorporated in the problem. The two-fold advantage of the approach taken here is that we obtain fault-independent solutions that can be used to control transient stability following a large range of faults, whilst also temporarily discarding some constraints that might have been limiting our understanding of the problem.

Obviously, the utility of our results is limited to post-fault states that are actually experienced in SMIB transient stability problems (ie. corresponding to realistic faults). However, by not *a priori* limiting our investigation to typical SMIB faults, we are also able to develop some new insights that have importance in the multi-machine transient stability problem.

1) *Infinite Horizon Discounted Cost*: The objective of the infinite horizon optimal design problem is to find the state-feedback control policy,  $u(x)$  for which  $u(x) \in \mathcal{U}$  for all  $x \in \mathbb{R}^2$ , that minimises the cost

$$J(x, u(x)) = \int_{t_c}^{\infty} h(x, u(x)) \exp(-\lambda t) dt \quad (3)$$

where  $\mathcal{U}$  is a bounded set of admissible control values,  $h(x, u) \geq 0$  is called the running cost and  $\lambda \geq 0$  is a discount factor. If  $h(x, u)$  is independent of  $u$ , then a bang-bang optimal solution will result.

Later, we will consider a variety of suitable cost functions including: minimum time optimal control (ie.  $\lambda = 0$ ,  $h(x, u) = 1$ ), and minimum energy control (ie.  $\lambda = 0$ ,  $h(x, u) = x'Rx$ ).

2) *Costs Suitable to SMIB problems*: Let us introduce  $\bar{\Omega}$  to denote the region of state space of interest in our stability study. We consider a bounded region (rather than all of  $\mathbb{R}^2$ ) because of limitations in our numeric technique. As long as we choose  $\bar{\Omega}$  large enough, our defined control problem will still represent our SMIB transient stability problem. Let us also introduce a target set containing the system equilibrium point, which we denote as  $\mathcal{T} \subset \bar{\Omega}$ . Then, in the control problems that follow, we will consider a running cost functions of the form

$$h(x, u) = \begin{cases} 0 & \text{if } x \in \mathcal{T} \\ \infty & \text{if } x \notin \bar{\Omega} \\ \bar{h}(x, u) & \text{otherwise.} \end{cases}$$

Now, let  $\Omega \subseteq \bar{\Omega}$  denote the subset of  $\bar{\Omega}$  from which stabilisation is possible. Our optimal control problem will determine  $\Omega$  (because unstable trajectories must leave  $\bar{\Omega}$ ). In particular, the stabilisable region will correspond to all  $x$  for which it is possible to find a  $u$  such that  $J(x, u)$  is finite.

*Remarks:*

- 1) The introduced control problem is a sensible problem (ie. is well posed) as long as  $\bar{h}(x, u) > 0$  for all  $x \in \bar{\Omega} - \mathcal{T}$ . This condition corresponds to requiring that the trajectory should eventually reach the target set or leave  $\bar{\Omega}$ .
- 2) There are a number of similar control formulations that may be useful for particular versions of the SMIB transient stability problem. For example, optimal stopping frameworks, optimal switching frameworks with switching costs or finite-horizon optimal control frameworks. See [1] for an introduction into various types of optimal control problems that may be suitable.

## B. The Dynamic Programming Solution to the Optimal Control Problem

Dynamic programming is a standard approach for finding optimal control solutions. As distinct from the ‘‘maximum principle’’ approach [11], the dynamic programming approach solves the optimal control problem for all the possible state values at once. That is, using dynamic programming we can solve for a range of faults and all fault durations in one step. Further, we will achieve a complete specification of the stability limits and determine the performance cost that will be achieved for any fault clearance time.

Moreover, dynamic programming solves the optimal control in state feedback form (rather than the open-loop form in which the ‘‘maximum principle’’ approach finds the solution). State feedback is generally considered more desirable because a state feedback controller can exploit the latest available information.

The ‘‘maximum principle’’ has previously been used in the context of SMIB transient stability [4], [8], [11], but we believe that this paper is the first time a dynamic programming solution to the problem has been presented.

Even though numeric techniques will be required to solve the presented SMIB transient control problem, it is useful to develop the analytic description of the problem as far as possible before we introduce a numeric approach.

The basis of the dynamic programming approach is the optimal cost function (known as the value function) defined as follows

$$v(x) = \min_{u(x) \in \mathcal{U}} J(x, u(x)). \quad (4)$$

This optimal cost function describes everything we need to know about this optimal control problem. Using dynamic programming, it can be shown that the optimal cost function for this problem is a solution (in a certain sense) to the following partial differential equation (PDE) :

$$\lambda v = H(x, Dv).$$

See [2] for complete details or [1] for an introduction. Here

$$Dv = \begin{bmatrix} \frac{\partial v}{\partial x_1} \\ \frac{\partial v}{\partial x_2} \end{bmatrix}$$

is the gradient of  $v$  and  $H(x, Dv)$  (which is called an Hamiltonian) is given by

$$H(x, Dv) = \min_{u \in \mathcal{U}} \left\{ \left[ M^{-1}(P_m - P_{max}(u) \sin(x_1)) \right] Dv + h(x) \right\} \quad (5)$$

where

$$P_{max}(u) = \frac{|E||V|}{X_{eff}(u)}.$$

This PDE involves mathematical concepts considerably outside the scope of this paper. Hence, it is not possible to provide a detailed explanation here. However, a few key observations are required at this point:

- 1) The importance of this PDE is that the optimal control policy is described by  $v(\cdot)$  (the  $u$  achieving the minimum in (5)).
- 2) When the running cost is independent of the control action, the optimal control is bang-bang.
- 3) In general, these PDEs cannot be solved in a closed form manner and numeric techniques must be used. This will be discussed in the next section.

### C. Numeric Solutions

As mentioned above, the PDE describing the optimal solution cannot generally be solved in an analytic sense. One technique for achieving a numeric approximation to the optimal control solution is the Markov chain approximation technique [3].

This approach is based on solving a different control problem whose solution converges to the optimal solution described by the PDE (4). In particular, this approach is not based on approximating the PDE directly. In fact, using the Markov chain approximation technique, the approximation can be developed without knowledge of the PDE.

In the Markov chain approach, the originally posed continuous time control problem is approximated by a discrete-time Markov chain control problem. By choosing the Markov chain control problem in a particular way, it can be shown that the approximate solution approaches the optimal solution to the originally posed problem.

The approach provided in [3] can be applied to this problem in a fairly routine manner.

## IV. POWER SYSTEMS EXAMPLES

In this section, we consider several power system transient stability problems that demonstrate the nature of the optimal solutions in this type of problem.

Unless noted, we consider a SMIB system with the following post-fault parameters (in pu):  $P_m = 0.9$ ,  $E = 0.90081$ ,  $V = 1.1626$ ,  $M = 0.0186$ ,  $u_{norm} = 0.7752$ ,  $u_{min} = 0.6752$ , and  $u_{max} = 0.8752$ . Here,  $u_{norm}$  is the nominal impedance and  $u_{min}$  and  $u_{max}$  are the lower and upper limits on the controllable impedance, respectively.

Let  $\delta_s = \sin^{-1}(P_m/P_{max}(u_{norm})) = 0.7291 \text{ rad}$ . Then, the system has a post-fault equilibrium (under constant  $u_{norm}$  control) at  $(\delta_s, 0)$ . A corresponding unstable equilibrium is at  $\bar{\delta}_s = \pi - \delta_s$ .

Throughout this section we will refer to a number of other key equilibrium points of the SMIB dynamics (all on the  $\omega = 0$  line). The stable and unstable equilibrium points under constant  $u_{min}$  control are denoted  $\delta_s^m$  and  $\bar{\delta}_s^m$ , respectively. The stable and unstable equilibrium points under constant  $u_{max}$  control are denoted  $\delta_s^l$  and  $\bar{\delta}_s^l$ , respectively (when they exist). All of these points are useful in describing the transient stability properties of controlled SMIB dynamics.

Typically, stability studies of power generation systems involve simulation of the system trajectories during the fault. However, using the above optimal control framework, we only required knowledge of the initial post-fault state to fully characterise the post fault behaviour. We note that faults on SMIB are typically cleared after the system state has evolved to somewhere in the  $\omega > 0$ ,  $\delta > \delta_s$  quadrant (or backswing to the  $\omega < 0$ ,  $\delta < \delta_s$  quadrant). However, in multi-machine stability problems, that use an equivalent SMIB model representation, it is possible for faults to be cleared after the state has evolved to other parts of the state-space (see the last provided example).

Once the optimal control problem has been solved, quantities such as the upper limit on acceptable clearing times for

particular types of fault can be easily found using a single simulation of the faulted system behaviour.

Using specialised code, the optimal control results shown below can be calculated by dynamic programming on a  $(160 \times 200)$  state-space grid in approximately 60 seconds of CPU time (on a 1GHz Pentium 3).

### A. Minimum Time Control

A minimum time control SMIB transient stability problem has been previously considered by others [4], [8]. In the framework presented in this paper, the minimum time control problem is a finite horizon control problem with  $\lambda = 0$  and  $\bar{h}(x, u) = 1$ .

Previous approaches have used the ‘‘maximum principle’’ approach to find closed-form optimal switching curves that solve the minimum time control problem [4], [8]. However, these previous solutions are developed under a number of implicit assumptions that do not fully characterise the SMIB transient stability problem (as demonstrated in Fig. 1).

Let us use the term the *marginally stable* region to denote the region where the fixed  $u = u_{min}$  control results in marginally stable trajectories. This region can be identified using energy methods (for example [5]). Previous results make no comment on stability issues outside this marginally stable region [4], [8].

Figure 1 shows the optimal solution (in feedback form) to the minimum-time transient stability problem for the above SMIB system. In this figure, at each  $(\delta, \omega)$  location there is either an optimal control action (be it  $u_{min}$  or  $u_{max}$ ) or the system cannot be stabilised from this state-space value (the outer region shown on the figure). Hence, this figure identifies both the stabilisable region and the optimal control within this stabilisable region. Note this figure is a plot of the numeric solution to the problem and contains several numeric artifacts, including: the non smooth nature of the boundary lines and the ‘‘double’’ lines between  $u_{min}$  and  $u_{max}$  regions due to the finite size of the approximation grid.

The system equilibrium point is at  $\delta_s = 0.7291 \text{ rad}$ , ie. where the ‘‘reverse s’’ shaped part of the switching curve crosses the  $\omega = 0$  line (see also remarks at the end of this section). The other possible stable equilibrium occur at  $\delta_s^m = 0.6190 \text{ rad}$  and  $\delta_s^l = 0.8513 \text{ rad}$  (corresponding to fixed  $u_{min}$  and  $u_{max}$  control respectively) which are roughly in the middle of each loop of the ‘‘reverse s’’ as shown in the figure. The unstable equilibrium are at locations  $\bar{\delta}_s^m = 2.5226 \text{ rad}$ ,  $\bar{\delta}_s = 2.4125 \text{ rad}$ , and  $\bar{\delta}_s^l = 2.2903 \text{ rad}$  corresponding to  $u_{min}$ ,  $u_{norm}$  and  $u_{max}$  respectively (the  $u_{max}$  unstable point is also marked on the figure).

Readers familiar with the switching curve solutions in previous approaches to the minimum-time transient stability problem can consider the boundaries between the  $u_{min}$  and  $u_{max}$  regions to be switching curves. We highlight that as suggested by the dynamics (1), the optimal bang-bang control swaps when  $\sin(\delta)$  changes sign.

Readers familiar with the velocity controller, for example [13], [14], should note that the  $\omega = 0$  switching line does not continue from  $\delta = 2.2903 \text{ rad}$  to  $\delta = 2.5226 \text{ rad}$  and hence

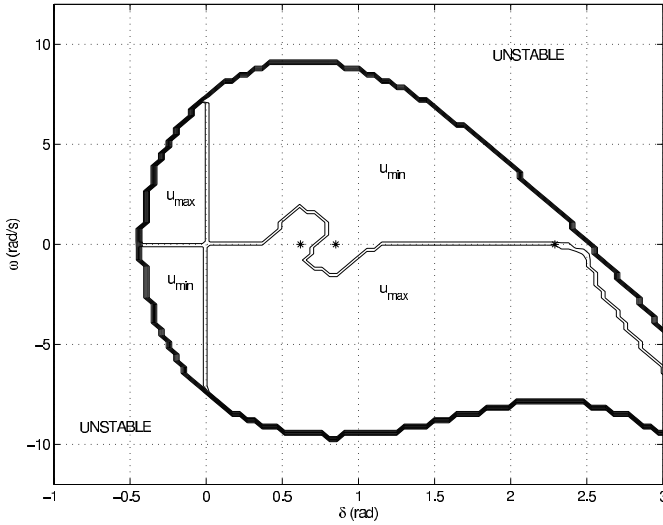


Fig. 1. Optimal switching to achieve minimum time control. The points  $\delta_s^m$ ,  $\delta_s^l$  and  $\bar{\delta}_s$  are marked by \*.

the controller of Fig. 1 will avoid the control chattering that can result in the previously identified “partially” stable region for  $\delta_s^l \leq \delta \leq \bar{\delta}_s^m$  [13].

The top part of the stability boundary (for  $\omega > 0$ ) is described by the top boundary of the marginally stable region while the boundary for  $\omega < 0$  is more complicated. For example part of the boundary (in the  $\omega < 0$  and  $\delta > \bar{\delta}_s^m$  region) is described by a reverse time trajectory from point  $(\bar{\delta}_s^m, 0)$ . The lower side of the stability boundary in this quadrant is determined by the reverse time trajectories under fixed control  $u = u_{max}$  that enter the marginally stable region.

Although not shown, the stabilisable region continues outside the region shown in the figure, in a direction described by reverse time trajectories under fixed control  $u = u_{max}$ . This corresponds to a region about the line described by (the  $w < 0$  part of the solution to):

$$\frac{1}{2}Mw^2 = P_m(\delta - \bar{\delta}) + \frac{|E||V|}{u_{max}} (\cos(\delta) - \cos(\bar{\delta})) \quad (6)$$

for some  $\bar{\delta}$ , where  $\bar{\delta}_s^l < \bar{\delta} < \bar{\delta}_s^m$ .

Figure 2 shows a sample stabilised trajectory that begins outside the marginally stability domain (the corresponding control sequence is shown in Fig. 3). The marginally stability region, as calculated by energy methods such as the PEBS method (see [5]), is shown on this figure as the region enclosed by the dashed line. This figure demonstrates that it is possible to stabilise the system from locations outside the marginally stable region. In this example, the control action is relatively small and many swings are required to achieve stability at the equilibrium point (this is different from the relative large control action cases considered in [4], [8]). Only the first 3.5 seconds of the minimum-time stabilised trajectory is shown.

Moreover, Fig. 3 illustrates that the required control sequence is not unreasonable (for example, does not involve chattering). However, other protection issues outside the scope of this paper may make this control approach undesirable.

The shape and nature of the stability domain in this problem will have important analogies in higher dimension, and these

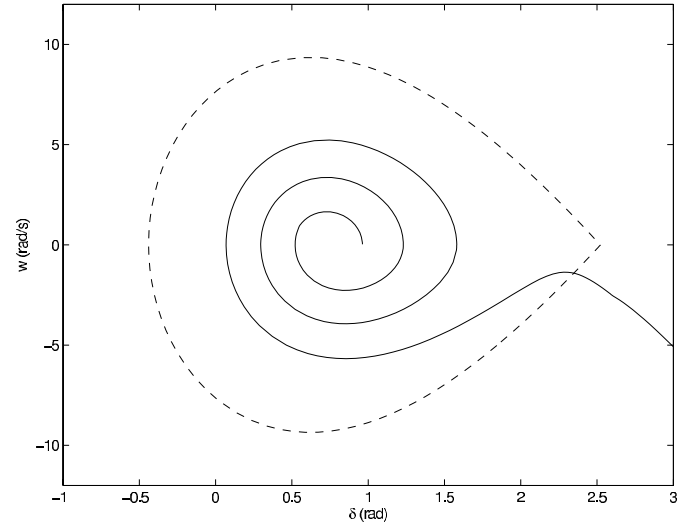


Fig. 2. One controlled trajectory (solid line) from within the stability domain (but outside the marginally stability region - boundary given by the dashed line). After the initial stage, the simulated trajectory is clockwise and ends after 3.5 seconds. Complete stabilisation to the equilibrium takes longer than 3.5 seconds. In principle, once within the marginal stability region, stabilisation to the equilibrium point is possible using a variety of control strategies: for example, our optimal control, minimum time control or velocity control.

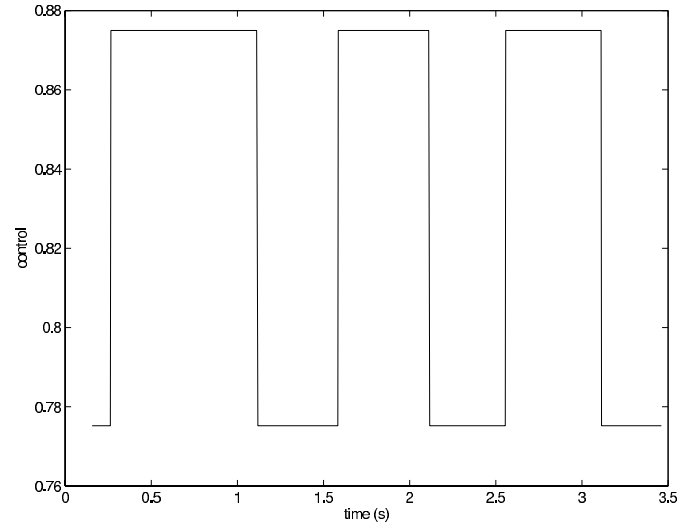


Fig. 3. The control sequence used to stabilise the trajectory.

concepts will aid understanding of the general angular separation problem. The nature of Fig. 1 suggests that the stability properties of the system should be understood in terms of at least 2 regions: the marginally stable region and another region.

### B. Example: Minimum Energy and Flicker Control

Let us consider the transient stability problem with respect to a criteria involving both energy and voltage flicker. In particular consider the same SMIB system with the following performance parameters:  $\lambda = 0$ ,  $\bar{h}(x, u) = \omega^2 + (\delta - \delta_s)^2 + 500(u - u_{norm})^2$ .

Note, the optimal control will not be bang-bang in this problem because the running cost contains a term dependent on the

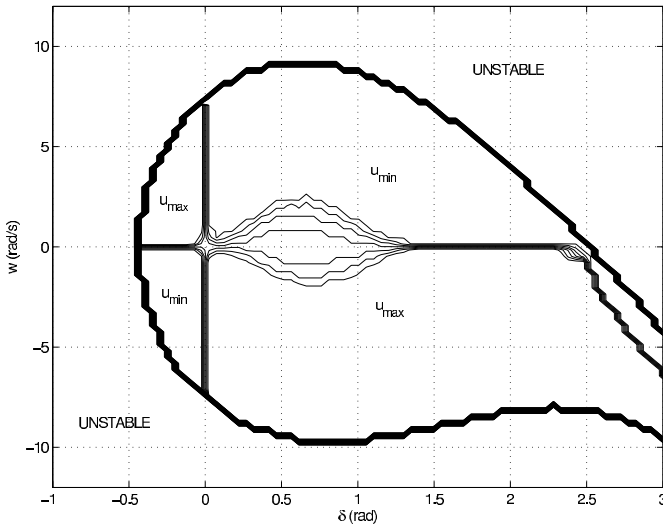


Fig. 4. Optimal control to achieve minimum energy and flicker control. The contour lines about the equilibrium point demonstrate that there is a gradual change between  $u_{max}$  and  $u_{min}$  when near the equilibrium.

choice of control action. In fact, near the system equilibrium, this control problem is almost a Linear Quadratic Regulation (LQR) problem and hence we might expect saturated linear controllers to be near optimal in this region (this matches the observations of [14] regarding the use of linear controllers for small disturbances and bang-bang for large disturbances). The optimal control solution is shown in Fig. 4.

The overall structure of the optimal solution in this problem is very similar to the minimum time solution shown in Fig. 1. In Fig. 4, the collection of lines near the system equilibrium point represent contours lines illustrating a gradual change between the  $u_{min}$  and  $u_{max}$  controls. Away from this equilibrium point, the optimal control is bang-bang. Hence, the optimal solution for this problem is bang-bang (when angular separation needs to be avoided), otherwise the size of the control effort is reduced (roughly like a saturated version of a linear state-feedback controller).

### C. Example: Larger Control and Minimum Energy

For completeness, let us consider a slightly modified transient stability problem in which larger control actions are available. Here consider the same SMIB dynamics, the above minimum energy criteria (without control cost) with controls  $u_{norm} = 0.7752$ ,  $u_{min} = 0.3752$ , and  $u_{max} = 1.1752$ .

The optimal control for this problem (shown in Fig. 5) retains the same basic structure with the stabilisable region increased and a distorted “reverse s” shape to the switching curve near the equilibrium. The system equilibrium point remains at  $\delta_s = 0.7291 \text{ rad}$ . The other stable equilibrium point is at  $\delta_s^m = 0.3283 \text{ rad}$  (corresponding to fixed  $u_{min}$ , in this example neither  $\delta_s^l$  nor  $\bar{\delta}_s^l$  exist). The unstable equilibrium are at  $\bar{\delta}_s^m = 2.8133 \text{ rad}$  and  $\bar{\delta}_s = 2.4125 \text{ rad}$  (corresponding to  $u_{min}$  and  $u_{norm}$  respectively).

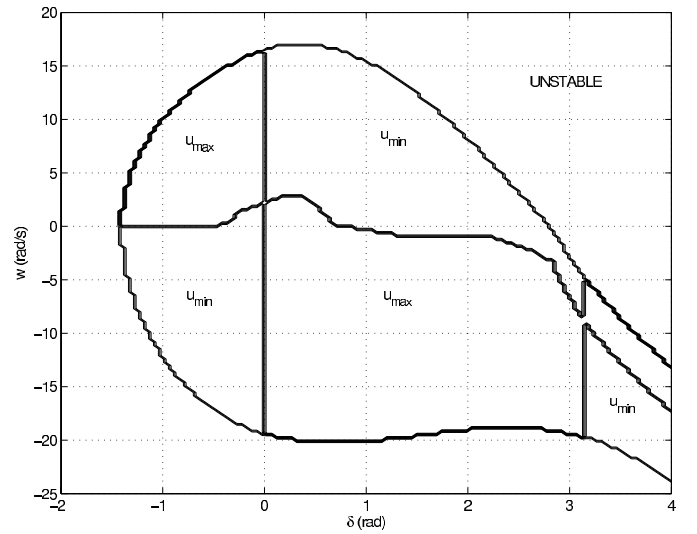


Fig. 5. Optimal minimum energy controller when larger controls are possible.

### Conclusions from SMIB Transient Stability Studies:

- 1) The velocity controller is a reasonable stabilisation approach.
- 2) A “partially” stable region exists above  $\bar{\delta}_s^l$ .
- 3) A saturated linear controller would also be a reasonable stabilisation approach.
- 4) Even in the SMIB case, existing energy methods do not fully characterise the transient stability problem. Stabilisation is possible from outside the marginal stability region.

### D. Example: Emergency Control of a Separating Light Machine

To demonstrate a potential utility of the extended stability regions of the above controllers, consider the three machine system shown in Fig. 6. In pu quantities, machine 1 is a heavy machine (with parameters  $P_{m1} = 0.9$ ,  $E_1 = 0.90081$ ,  $M_1 = 0.2790$ ), machine 2 is a light machine (with parameters  $P_{m2} = 0.8$ ,  $E_2 = 0.90081$ ,  $M_2 = 0.0027$ ), and the third machine represents the rest of the power system as an infinite bus at  $V = 1.1626$ . Denote the three links as  $L_{1B}$ ,  $L_{2B}$ , and  $L_{12}$ . We assume link  $L_{1B}$  and  $L_{12}$  have a purely reactive impedances of 0.7752 and 1.5504, respectively. Finally, we assume link  $L_{2B}$  contains a series compensation device providing controllable impedance between  $u_{min} = 1.3954$  and  $u_{max} = 1.7054$ . We denote the nominal impedance of link  $L_{2B}$  as  $u_{norm} = 1.5504$ .

Prior to the fault, machine 1 and machine 2 are at the equilibriums ( $0.9321 \text{ rad}, 0$ ) and ( $1.1456 \text{ rad}, 0$ ), respectively.

A fault to ground occurs on link  $L_{2B}$  and is cleared after 0.1 seconds. If no control is utilised, then the heavy-light combination of machines will undergo multi-swing instability and angular separation occurs on the second swing. If protection relays on the  $L_{12}$  link are triggered earlier enough (within one swing) the heavy machine can be saved from separation (but the light machine will separate).

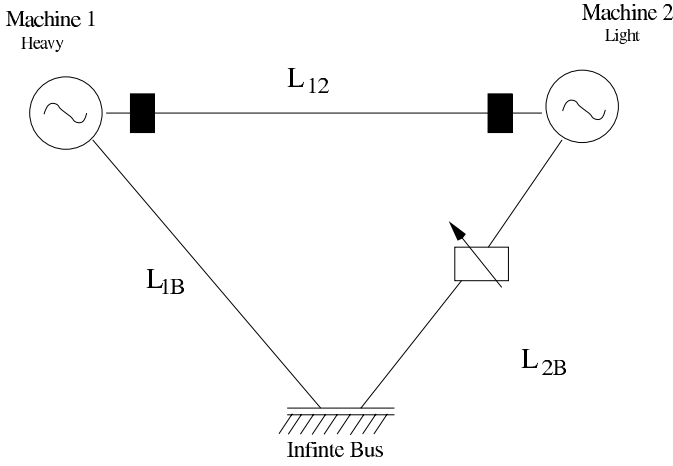


Fig. 6. A heavy-light three machine example with a significant risk of separation.

Consider an SMIB analysis of the post-fault behaviour of the light machine. Let  $\delta_s^m = \sin^{-1}(P_{m2}/P_{max}(u_{min}))$  denote the only possible post-fault equilibrium for the light machine (if  $L_{12}$  link is isolated). However, the initial post-fault trajectory of the light machine has  $\delta > \delta_s^m$  where  $\bar{\delta}_s^m = 1.8964 \text{ rad}$  is the critical clearing angle given by the equal area criterion. This might suggest that stabilisation of the light machine is not possible, either with or without isolation of link  $L_{12}$ .

Yet, if the timing of the protection relays on link  $L_{12}$  can be co-ordinated with the control on link  $L_{2B}$ , then separation of both machines can be avoided by utilising the extended stability region of the controllers presented above. A key realisation is that switching to  $u_{max}$  should occur on (or near) the line

$$\frac{1}{2}M_2w_2^2 = P_{m2}(\delta - \bar{\delta}) + \frac{|E_2||V|}{u_{max}} (\cos(\delta) - \cos(\bar{\delta})) \quad (7)$$

for some suitable  $\bar{\delta} < \bar{\delta}_s^m$ . In this problem,  $\bar{\delta}_s^l$  does not exist (because  $u_{max}$  is unstable) so it is possible to choose  $\bar{\delta}$  near the desired equilibrium point  $\delta_s^m$ . Hence, stabilisation within a single swing is possible.

Figure 7 shows the stabilised trajectory achieved for machine 2 (the light machine). Fault clearance occurs at point A ( $t = 0.1 \text{ s}$ ). At point B ( $t = 0.238 \text{ s}$ ) the post-clearance trajectory crosses the line (7) and the protection relays on  $L_{12}$  are triggered. At the same time, the control  $u = u_{max}$  is applied on link  $L_{2B}$ . The trajectory evolves from point B towards the equilibrium in a similar manner to the behaviour exhibited in our minimum-time example, Fig. 2. With the protection relays on link  $L_{12}$  being triggered at point B, machine 1 will remain within its marginal stability limits without further control (hence, machine 1 trajectories are not shown here). Once the trajectory is near the equilibrium for machine 2 (at  $t = 0.372 \text{ s}$ ), the control  $u_{min}$  is applied and the system will be marginally stable until the link  $L_{12}$  is restored (that is, will exhibit a trajectory cycle about, rather than stabilise to, the equilibrium point). Once link  $L_{12}$  is restored, it will be possible to stabilise the three machine system to the pre-fault equilibrium.

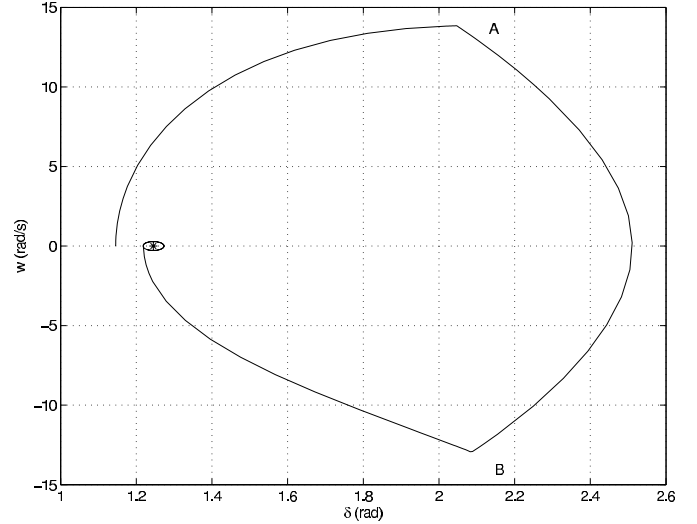


Fig. 7. A trajectory demonstrating stabilisation of a light machine at risk of separation. Fault clearance occurs at point A. At point B, the protection relays on  $L_{12}$  are triggered, and control  $u = u_{max}$  is applied on link  $L_{2B}$ . Near the equilibrium, control  $u = u_{min}$  is applied and marginally stability behaviour occurs. That is, a trajectory cycle around the equilibrium point occurs until further stabilisation can be achieved after the restoration of link  $L_{12}$ . The size of the trajectory cycle is related to the timing accuracy of the control actions.

The control sequence to achieve the stabilisation shown in Fig. 7 involves only 2 switches and would be reasonable to implement. However, the control scheme requires reasonable timing information in the sense that event B must be trigger somewhere between  $t = 0.230 \text{ s}$  and  $t = 0.245 \text{ s}$  to achieve marginal stability of the light machine.

During the period that the protection relays are isolating link  $L_{12}$ , machines 1 and 2 have new equilibrium. Machine 2's new equilibrium is at  $\delta_s^m = 1.2452$  as can be seen in Fig. 7. Note also that machine 2 is not stable under control  $u = u_{norm}$  during the period in which link  $L_{12}$  is isolated (that is, the link impedance must be held at  $u_{min}$ ). Hence, following the time period shown in Fig. 7, link  $L_{12}$  will need to be restored in a timely manner so the system can be returned to the pre-fault equilibrium.

Finally, we remark that if link  $L_{12}$  also contains a controllable compensation device, then this additional control device will also aid stabilisation of the light machine.

For completeness, the above 3 machine system is stable for  $t_c < 0.95 \text{ s}$ , multi-swing unstable for  $0.95 \text{ s} \leq t_c \leq 1.2 \text{ s}$  and first-swing unstable for  $t_c > 1.2 \text{ s}$ . Hence, the presented control design approach can increase the critical clearing time in this example from  $\bar{t}_c = 0.95 \text{ s}$  to  $\bar{t}_c = 1.2 \text{ s}$ .

#### Remarks:

- 1) There are two things to note about the ‘‘reverse s’’ part of the switching curve in Fig.1. Firstly, this ‘‘reverse s’’ shape also appears near the equilibrium in the previous time-optimal solutions to the transient stability problem, in particular see [8]. The ‘‘reverse s’’ in Fig. 1 is small because only small control actions are available in this example. Secondly, this part of the switching curve has almost no impact on the achieved performance and replacing this ‘‘reverse s’’ curve (near the system

equilibrium) with the  $\omega = 0$  line will have no noticeable impact on the performance achieved.

## V. CONCLUSIONS

In this paper we have solved a SMIB transient stability problem using the dynamic programming approach to non-linear optimal control. Unfortunately, the optimal solution does not have a closed form solution, so a numeric approximation technique is identified and then demonstrated on several examples.

By examining the most general solution to the SMIB transient stability problem, the merit and limitations of previously proposed approaches can be understood within a single framework. The presented examples help to more rigorously demonstrate a number of existing ideas, but also to identify a number of new concepts that improve our understanding of the transient stability problem.

## REFERENCES

- [1] D.P. Bertekas, *Dynamic Programming and Optimal Control*, Vol. 1 & 2, 2nd Ed., Athena, Massachusetts, 2000.
- [2] M. Bardi and I. Capuzzo-Dolcetta, *Optimal Control and Viscosity Solutions of Hamilton-Jacobi-Bellman Equations*, Birkhauser, Boston, 1997.
- [3] H.J. Kushner and P. Dupuis, *Numerical Methods for Stochastic Control Problems in Continuous Time*, 2nd Ed., Springer, New York, 2001.
- [4] D.N. Kosterev and W.J. Kolodziej, "Bang-Bang series capacitor transient stability control", *IEEE Trans. on Power Systems*, Vol. 10, No. 2, pp. 915-924, May 1995.
- [5] M.A. Pai, *Energy function analysis for power systems stability*, Klumer Academic Publishing, Boston, 1989.
- [6] M. Pavella, D. Ernst, D. Ruiz-Vega, *Transient stability of power systems: a unified approach to assessment and control*, Klumer Academic Publishing, Boston, 2000.
- [7] D.K. Reitan and N. RamaRao, "Pontryagin's Maximum Principle Aids Transient Stability: Bang-Bang Control of Reactance", *Proceedings of the IEEE*, pp. 1734-1735, Oct. 1968
- [8] J. Chang and J.H. Chow, "Time-optimal control of power systems requiring multiple switchings of series capacitors", *IEEE Trans. on Power Systems*, Vol. 13, No. 2, pp. 367-373, 1998.
- [9] J. Peng, Y. Sun and H.F. Wang, "Co-ordinated emergency control of generator-tripping and SMES based on Hamiltonian system theory", *Electrical Power and Energy System*, Vol. 27, pp. 352-360, 2005.
- [10] T. Kato, K. Yukita, Y. Goto, K. Ichiyonagi, Y. Tabata, and S. Ogawa, "A study of switching technology using serial and parallel resistors for power systems stabilization", *Electrical Engineering in Japan*, Vol. 142, No. 2, pp. 59-67, 2003.
- [11] M.M. Gavrilovic, "Optimal control of SMES systems for maximum power system stability and damping", *Electrical Power & Energy Systems*, Vol. 17, No. 3, pp. 199-205, 1995.
- [12] J. Peng, Y. Sun and H.F. Wang, "Co-ordinated emergency control of generator-tripping and SMES based on Hamiltonian system theory", *Electrical Power and Energy Systems*, Vol. 27, pp. 352-360, 2005.
- [13] T. Chan, G. Ledwich and E.W. Palmer, "Is velocity feedback always best for machine stability control?", Aupec 2002, Melbourne, Australia, Oct. 2002 (Available at [www.itec.uq.edu.au/aupec/aupec02/Final-Papers/T-W-Chan1-808.pdf](http://www.itec.uq.edu.au/aupec/aupec02/Final-Papers/T-W-Chan1-808.pdf)).
- [14] M.R. Haque, "Application of energy function to assess the first-swing stability of a power system with a SVC", *IEE Proc. Gener. Transm. Distrib.*, Vol. 152, No. 5, Nov. 2005, pp. 806-812.

the Australian Defence Science and Technology Organisation. His current research interests include transient stability and emergency control of power systems, control of differential-algebraic systems, non-linear optimal control and dynamic programming.

**Gerard Ledwich** (M'73, SM'92) is a Chair Professor in Electrical Asset Management in the Queensland University of Technology, Australia (sponsored by the Transmission and Distribution companies of Queensland). He has held this position since Dec. 1998. In 1976 he received a Ph.D. in EE from the University of Newcastle, Australia. His interests are in the areas of Power Systems, Power Electronics and Controls. He is a Fellow of I.E. Aust.

**Zhao Yang Dong** (M' 99) received his PhD in Electrical and Information Engineering from the The University of Sydney, Australia in 1999. He is now a senior lecturer at the School of Information Technology and Electrical Engineering, The University of Queensland, Australia. His research interests include power system security assessment and enhancement, electricity markets, and artificial intelligence and its application in electric power engineering.

**Jason Ford** was born in Canberra, Australia, in 1971. He received BSc, BE and PhD degrees from the Australian National University (in 1995, 1995 and 1998 respectively). He is currently a Research Fellow at the Queensland University of Technology. Previously he has held positions at the University of New South Wales at the Australian Defence Force Academy and at